ORIGINAL PAPER

Greener production of silver nanoparticles: a sensitive nanodrop spectrophotometric determination of biothiols

Varsha Chandrakar[1] · Kavita Tapadia[1] · Saurabh Kumar Gupta[1]

Abstract

In the present work, we report an environmentally friendly, low cost, rapid, biocompatible, and greener approach for the production of silver nanoparticles (AgNPs) via the latex extract of *Ficus benghalensis*. The latex extract contains bioactive phytochemical constituents that can reduce and stabilize the silver salt in reacting solution. The resulting AgNPs were characterized. The surface plasmon resonance (SPR) was measured at wavelength, λmax 410 nm. High resolution transmission electron microscopy (HR-TEM) and scanning electron microscopy of AgNPs revealed the spherical shape with mean particle size was approximately 14 ± 0.69 nm. AgNPs Capped with latex show a strong affinity to the thiol group of biothiols (L-cysteine and glutathione). Upon the addition of biothiols, the absorbance of AgNPs decreased with a new SPR peak appeared at a higher wavelength, suggesting that the AgNPs were conjugate to biothiols with rapid aggregation. Owing to this interaction, a nanodrop spectrophotometer (NDS) was used as an advanced, fast response, and high-efficiency colorimetric assay for the selective determination of L-cysteine (Cys) and glutathione (GSH). A good linear relationship was found over the range of 0.2–1.0 ppm of biothiols. The obtained detection limits (LOD) were 0.17 and 0.18 ppm for the Cys and GSH, respectively. The applicability of the proposed NDS procedure has been validated by determining Cys and GSH in biological samples with satisfactory recovery results.

Graphic abstract
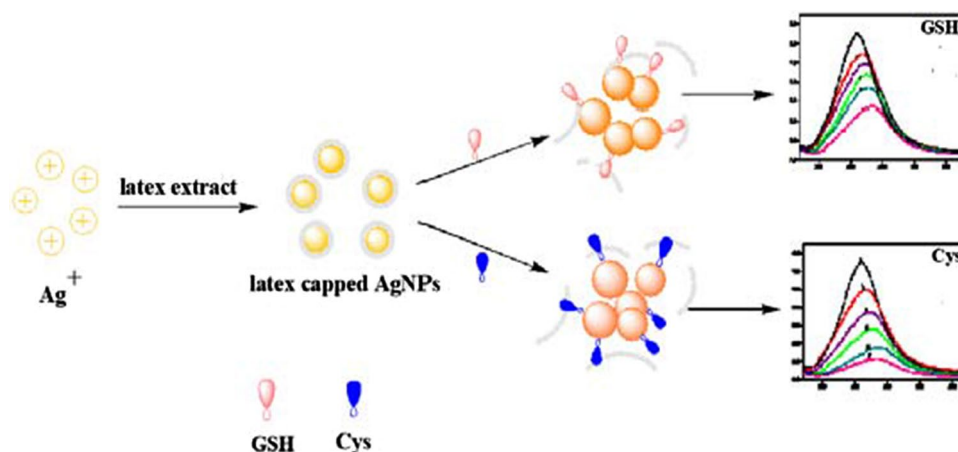
Keywords Green synthesis · Silver nanoparticles · Latex · L-Cysteine · Glutathione · Nanodrop spectrophotometer

✉ Kavita Tapadia
  ktapadia.chy@nitrr.ac.in

[1] Department of Chemistry, National Institute of Technology, Raipur, Chhattisgarh 492010, India

Introduction

Nowadays, nanoparticle research is being much important not only due to the application but also the path of synthesis (Ibrahim 2015). The development of greener production of metal nanoparticles is a viable option for chemical and physical procedures as it eliminates the use of toxic, expensive, and potentially harmful chemicals (Song et al. 2009). The flavonoids in plant extract not only act as powerful reductant but also provide the natural source pathway for the stabilization of nanoparticles (Aromal et al. 2012; Patra et al. 2015).

Over the last few decades, silver nanoparticles (AgNPs) have gained global consideration owing to their widespread applications. In a few experimental reports, the different approaches are documented, for the successful production of AgNPs from different plant's part as a leaf (Rout et al. 2012), fruit (Vishwasrao et al. 2019), bark (Sathishkumar et al. 2009), and peel of fruit (Kahrilas et al. 2014) by the selection of biocompatible capping for the stabilization (Potesil al. 2005). Many researchers also have shown their interest in the biosynthesis of AgNPs from fungus (Verma et al. 2010), vitamins (Nadagouda and Varma 2008), and polysaccharides (El-Rafie et al. 2013). However, these processes take a longer reaction time (4–24 h), severe extraction processes, operating at high temperature, and require culture preparations.

Ficus benghalensis plant is known as the Indian Banyan tree (Sharma et al. 2009). The latex extract of *F. benghalensis* is composed of a variety of alkaloids, flavonoids, and Phenolic compounds (Yadav et al. 2011). Hydroxyl (–OH) and keto (> C=O) groups in these compounds are capable to bind with metals and show high nucleophilic character and can donate an electron and reduce metal salt to form nanoparticles (De Matos et al. 2011).

L-Cysteine (Cys) and Glutathione (GSH) are low molecular weight amino acids having –SH moiety (biothiols) found in Human plasma and urine (Bahram et al. 2014; Hormozi et al. 2012). Cys are usually formed in the liver and involved in many physiological processes including protein synthesis and metabolism (Li et al. 2014; Ravindran et al. 2012). GSH is a strong antioxidant that is wildly present in animal tissues and involved in cell growth and division, catabolism, and detoxification of drugs (Deng et al. 2011; Huang et al. 2009; Li et al. 2017). Abnormal levels of these biothiols caused renal diseases, liver damage, hair depigmentation, diabetes, HIV disease, and skin lesion (Detsri and Seeharaj 2017; Raj et al. 2017; Raoof et al. 2008; Yuan et al. 2013;). Therefore, accurate monitoring of Cys and GSH is important to diagnose the diseases at an early stage. Due to simplicity and high sensitivity, spectrophotometer probes are a powerful tool for monitoring trace amounts of analytes in the sample.

Up to now, several techniques are available for the detection of biothiols such as HPLC (Potesil et al. 2005; Rahman et al. 2006), electrochemical (Hsiao et al. 2011; Siddiqui et al. 2017), chemiluminescence (Yang et al. 2008), voltammeter (Vinoth et al. 2017), LC/MS (Guan et al. 2003; Alothman et al. 2013), Fluorescence (Amjadi et al. 2015) methods have been developed. Although these techniques showed promising results, unfortunately, they have some disadvantages such as longer analysis time, expensive, and tedious sample preparations. Therefore, it is needs to develop a low cost, rapid response, more precise, and accurate strategies for the detection of biothiols.

Nanodrop spectrophotometer (NDS) is a modern and relatively new rapid reading technique, which eliminates the need for cuvettes; therefore, this instrument employs the shorter path length (only 1–2 mm path length) to occur in a short time and minimal volume (0.5–1.0 µL) of sample required for determination (Desjardins et al. 2009).

Herein, we have explored a natural attempt for the rapid production of AgNPs using *F. benghalensis* latex extract as a reducing and protecting agent. The prepared AgNPs were confirmed by different characterization tools. We also studied and analyzed the interaction between biothiols (Cys and GSH) and AgNPs to determining Cys and GSH content in biological samples such as human blood and urine via novel and advanced NDS measurement. During experimental work, all optimum conditions were analyzed.

Experimental

Material

Chemicals

Silver Nitrate (AgNO$_3$, 99.8%) was purchased from Sigma-Aldrich. Hydrochloric acid (HCl, 38%), sodium hydroxide (NaOH, 99.5%), and sodium chloride (NaCl, $\geq$ 99.5%) were obtained from Merck. L-cysteine (Cys, $\geq$ 99%) and glutathione (GSH, $\geq$ 99%) and other amino acids were from Loba Chemicals, PVT Ltd. (Mumbai, India). All the chemicals are analytical reagent grade. The 10 ppm working stock solutions of biothiols were prepared by appropriate dilution.

Instrumentation

Characterizations were performed by Nanodrop (Thermo scientific-1000), full-spectrum (220–750 nm) spectrophotometer, SEM (FEI- Quanta-200 USA) operating at 40 kV, EDX (JED-2300) instrument coupled with SEM unit, HR-TEM with (JEM-2100F, JEOL Ltd, Tokyo, Japan) operating at 200KeV. IR analysis was carried out using the KBr pellets in the range

of 4000–400 cm^{-1} on FTIR (Thermo Nicolet, Avatar 370 model, Thermo scientific, USA).

Preparation of latex aqueous extract

Crude white milky latex obtained from the stem of *F. benghalensis* (NIT campus, Raipur, CG, India). Latex from *F. benghalensis* was collected in the early morning. In a reaction method, 3.0 ml latex was diluted to 100 ml using double distilled water to make it 3% and centrifuged twice at 10,000 rpm for 20 min. After centrifugation, latex constituting the aqueous fraction was separated from the precipitated rubber. The aqueous fraction was stored at 4 °C for further synthesis of AgNPs.

Synthesis of AgNPs

Separately, 5.0 ml of 3% latex aqueous extract and 10 ml of 1.0 mM AgNO$_3$ solution were heated at 60 °C with continuous stirring for 20 min in a water bath. The AgNO$_3$ solution was removed from the heating mantle and kept in an ice bath. Then 5.0 ml of latex extract was added drop wise with vigorous stirring until brownish-yellow color appeared which indicates the synthesis of AgNPs. The prepared AgNPs were stored at 4 °C in the refrigerator until further use.

Analytical processes for the determination of Cys and GSH

For biothiols detection, take 800 μL of as-prepared AgNPs in 1.0 ml sample vial. To this solution, 100 μL of different concentrations (0.2–1.0 ppm) of Cys were added; one by one in order, and then the solutions were diluted with double distilled water to 1000 μL. The same procedure was applied for GSH. The pH was adjusted to 5.8 for Cys and 5.0 for GSH with 0.1 M of HCl and NaOH. Then the solutions were agitated for 5 min by a vortex shaker. Absorption spectra of final mixture were recorded using NDS against reagent blank at λmax 410 nm.

A similar analytical procedure with slight modification was carried out for the determination of biothiols in human blood and urine samples, according to the standard addition method and detected by nanodrop spectrophotometer. All sets of analyses were repeated in triplicate. Biological samples were collected from the Private Pathology Laboratory, Raipur (CG).

Result and discussion

Absorption studies

Absorption spectra for latex extract and AgNPs are displayed in Fig. 1. The reduction of Ag$^+$ ion to AgNPs may be

optically approved by color changes of the starting material from colorless to brownish-yellow color. The formation of AgNPs was examined by NDS with distinct surface plasmon resonance (SPR) around 410 nm. The position of absorption spectra of AgNPs is strongly dependent upon the particle size (Saeb et al. 2014). One single peak absorption spectra show the spherical shape of nanoparticles (Bawaskar et al. 2010). The absorbance of AgNPs was taken again after 24 h. No obvious change in absorbance was noticed during storage, indicating that the AgNPs are stable.

FTIR/ functional group studies

The FTIR spectra of the latex extract and latex capped AgNPs are given in Fig. 2. The absorption peak of latex extract at 3445 cm^{-1} (may be attributed to O–H stretching of phenols, alcohols, and carboxylic acid) shifted toward lower wavenumber 3370 cm^{-1} upon binding with silver, signify to the involvement of the reduction process. The peak shifted from 2903 to 2850 cm^{-1} corresponds to the vibration of C–H stretching and the peak at 1625 cm^{-1} shifted to 1590 cm^{-1} corresponds to carbonyl stretch vibration in ketones, carboxylic acid, and aldehydes.

The peak at 1411 and 1390 cm^{-1} may assign to aromatic vibration. Other peaks visible in both spectra are 1060, and 1009 cm^{-1} indicates the stabilization of AgNPs by flavonoids, alkaloids, and Phenolic compounds present in latex extract.

SEM /surface morphology—EDX/elemental analysis

SEM was employed to analyse the shape of nanoparticles. Figure 3a presents the spherical shape of AgNPs with the nanoscale range. EDX analysis gives the elemental composition at a specific location which involved in the synthesis of
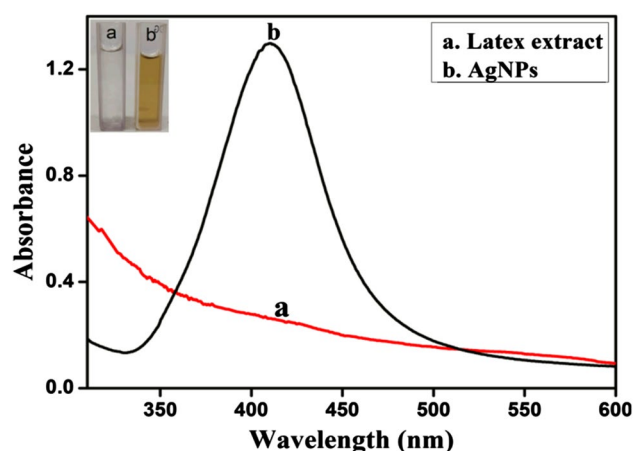

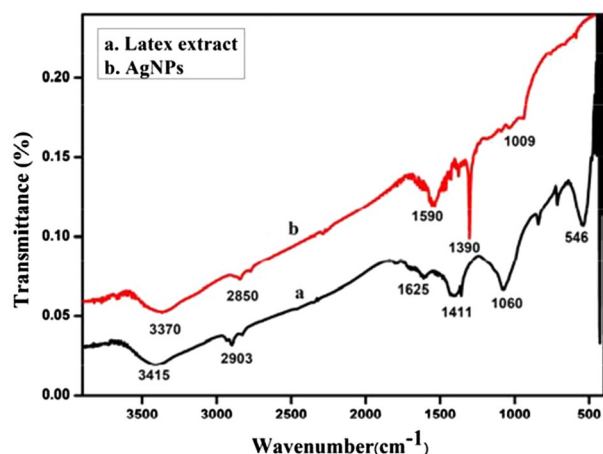**Fig. 1** Absorption spectra of **a** Latex extract and **b** Latex capped AgNPs

Fig. 2 FTIR analysis of **a** latex extract and **b** latex capped AgNPs

nanoparticles (Khan et al. 2016). The EDX spectrum demonstrates the presence of a high percentage value for silver at 3 eV, and its amount was founded to be nearly 77.53% as shown in the table embedded inside the curve as demonstrated in Fig. 3b. Other element signals including C and O are present possibly due to elements from capping agents present on the surface of AgNPs.

HR-TEM/size analysis

The HR-TEM micrographs provide information about the morphology and the average size distribution of nanoparticles. The AgNPs without biothiols were mostly spherical in morphology and well dispersed with an average size of 14 ± 0.69 nm as demonstrated in Fig. 4a. After the addition of biothiols, it is clearly shown that AgNPs aggregated with bigger sizes as shown in Fig. 4b and c. The mean

size of particles was 24.7 ± 0.64 nm to AgNPs-Cys and 21.2 ± 0.49 nm to AgNPs-GSH, obtained by histogram as indicated in Fig. 4. The results were shown as mean $\pm$ standard error (SE).

To obtain the optimum analytical conditions for the determination of biothiols affecting variables, including pH of the solution, incubation time and ionic strength have been evaluated.

Effect of pH

Figure 5a showed the pH effect on the detection of biothiols, which can be attributed to the interaction between thiol and AgNPs. The experimental results show that the optimum pH is 5.0 for GSH, and 5.8 for Cysteine. Therefore, pH 5.8 and 5.0 were chosen for Cys and GSH, respectively, for further studies. The error bar corresponds to the standard deviation of three repeated measurements.

Incubation time

Absorption spectra of AgNPs were taken at different time intervals (1–8 min) after the addition of biothiols at room temperature as given in Fig. 5b. The colorimetric performance was accomplished at 5 min, and beyond this, the absorbance of AgNPs-thiol conjugates remained constant. Based on these results, 5 min was selected as the optimal reaction time in our experiments.

Effect of AgNPs concentration

The effect of AgNPs concentration for the determination of biothiols was optimized. Figure 5c showed the evolution of absorbance upon adding 0.2 ppm of biothiols to different volume of AgNPs (200–1000 µL). It was found that the
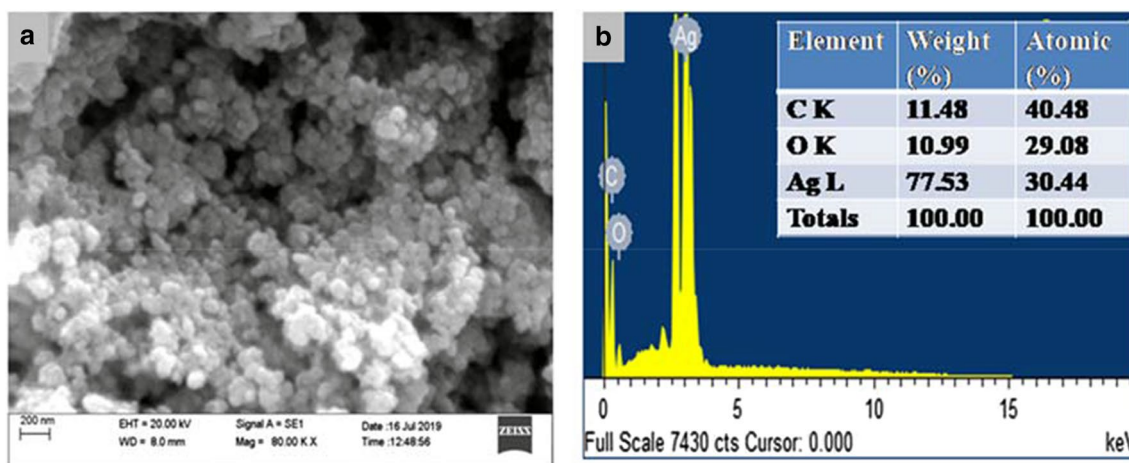

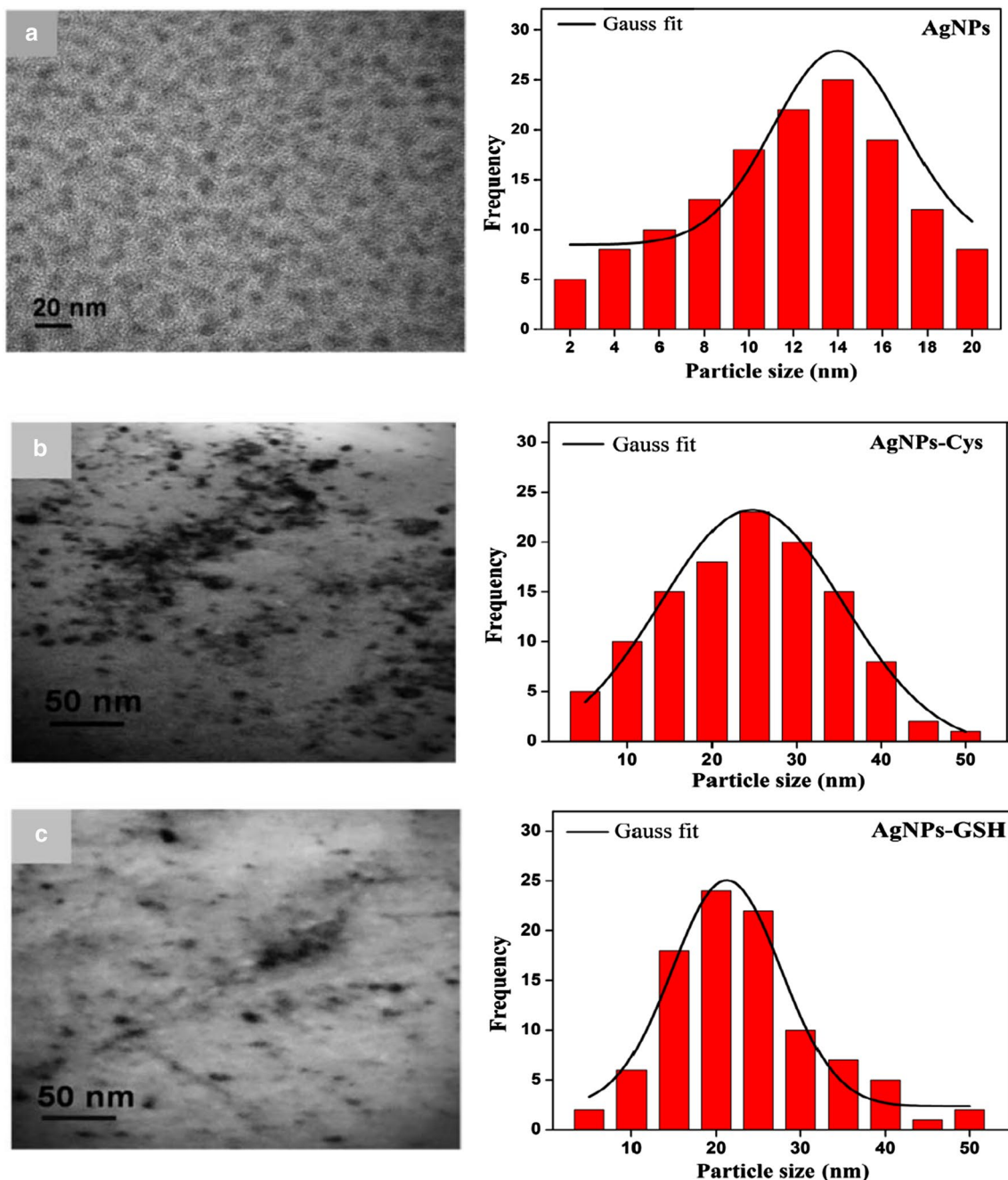**Fig. 3** **a** SEM and **b** EDX images of latex capped AgNPs

Fig. 4 Representative HR-TEM micrographs of **a** latex capped AgNPs, **b** AgNPs-Cys, and **c** AgNPs-GSH, and their corresponding particle size distribution histogram derive from HR-TEM micrographs

absorbance increased with increasing the concentration of Latex capped AgNPs and reached the maximum when 800µL was used. Therefore, 800 µL was used as the optimized volume.

Effect of ionic strength

The intensity of AgNPs-biothiol was measured in the presence of NaCl as demonstrated in Fig. 6a. The addition of

NaCl does not show any obvious changes in the position of absorbance maxima and the shape of the spectra of AgNPs-biothiol conjugates.

Selectivity studies

Importantly, to highlight the selectivity of the proposed method, latex capped AgNPs are independently exposed to 1.0 ppm other biomolecules in absence of biothiols. This
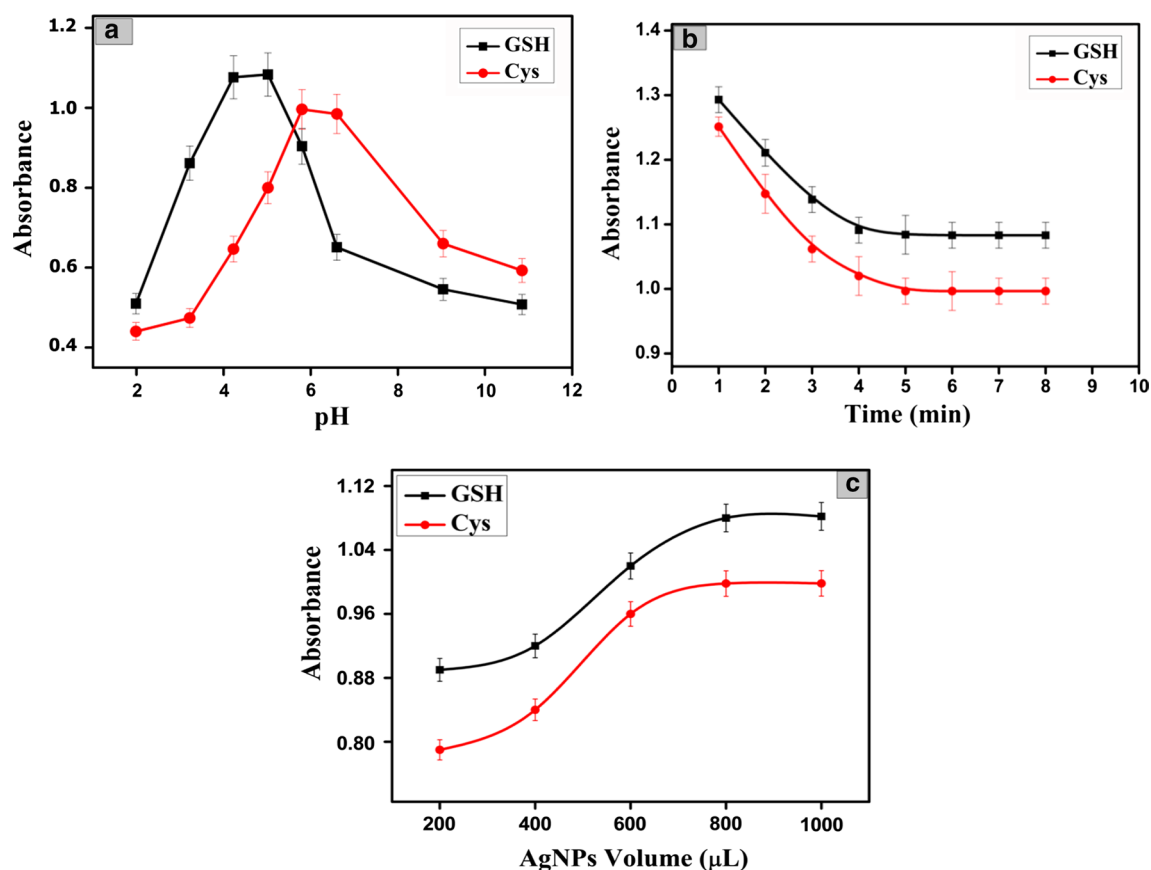
Fig. 5 a Effect of pH on interaction of Cys and GSH with AgNPs b Incubation time c Effect of AgNPs concentration under optimized reaction condition
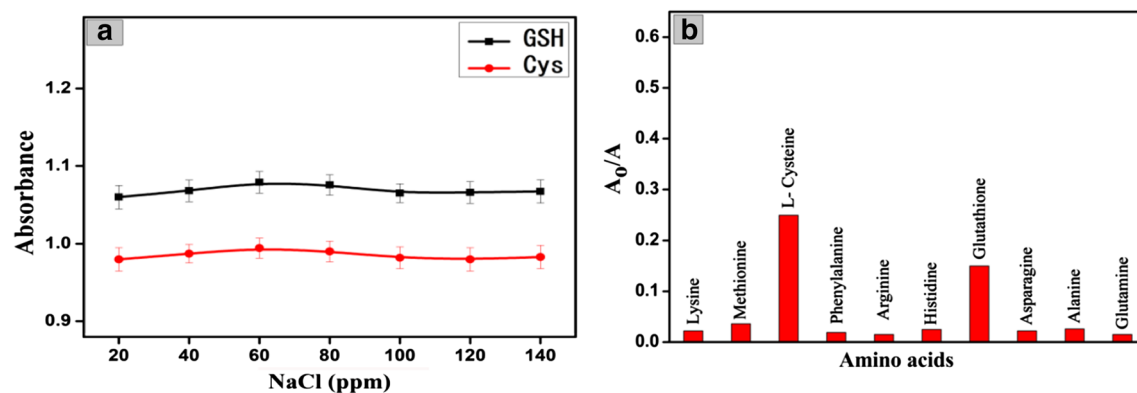

Fig. 6 a Effect of NaCl (20–140 ppm) on biothiol-AgNPs conjugates under optimized condition, b The absorbance ratio (A_0/A) of AgNPs mixed with Cys, GSH and other amino acids, where Ao and A is absorbance of AgNPs before and after the addition of amino acid, respectively.

investigation revealed that a wide range of other biomolecules did not exhibit significant optical responses due to lack of thiol group. But in presence of just 0.2 ppm of Cys and GSH, separately, the intensity ratio is higher comparison to other amino acids are given in Fig. 6b.

Analytical performance of AgNPs with biothiols

Remarkably, we observed owing to the strong affinity of thiol to AgNPs, biothiol will replace the adsorbed capping molecules and be easily bind to the surface of AgNPs. The

size, shape, composition, and aggregation state of particles always result in the change in wavelengths and absorbance maxima (Bahram et al. 2014). On the addition of increasing aliquot of biothiol to AgNPs, the SPR peak shifts to higher wavelengths and a significant decrease in the absorbance with broadening. Based on such observation, it can be concluded that the AgNPs were aggregated, and their size gradually increased with increasing concentration of biothiols as given in Figs. 7a and 8a.

To estimate the sensitivity of latex capped AgNPs for detection of biothiols, normalized absorbance was monitored as a function of biothiols concentration as shown in Fig. 7b and 8b. The calibration curve was obtained as a linear graph with regression coefficient (R^2) 0.9912 and 0.9921 for Cys and GSH, respectively. The normalized absorbance was calculated as $\Delta A/A_0$ ($\Delta A = A_0 - A$), where A_0 and A were the absorbances of AgNPs before and after the addition of biothiols, respectively. The limits of detection (3σ) for Cys and GSH were 0.17 ppm and 0.18 ppm, respectively (Christian 2007). The estimated LOD values for Cys and GSH are more

significant compared with other reported approaches using as given in Table 1.

Application

To assess the applicability of nanodrop spectrophotometric strategy for real sample analysis, known concentrations of Cys and GSH were spiked with biological fluid samples (Human blood and urine) by triplicate analysis ($n = 3$). The proposed method was validated with the outcomes of satisfactory recoveries, 91.33%-98.75% with RSD 0.92–1.13% for Cys and 91.65–96.00% with RSD 0.91–1.45% for GSH, confirming that our methodology is highly reproducible. The results are listed in Tables 2 and 3. The performance of the proposed method is also compared with those obtained by reference method with regard to t value and F value at 95% confidence level (Kalaiyarasan et al. 2019; Liang et al.2002; Mohammadi et al. 2017). From the table, we found that the calculated t and F value were smaller than its corresponding
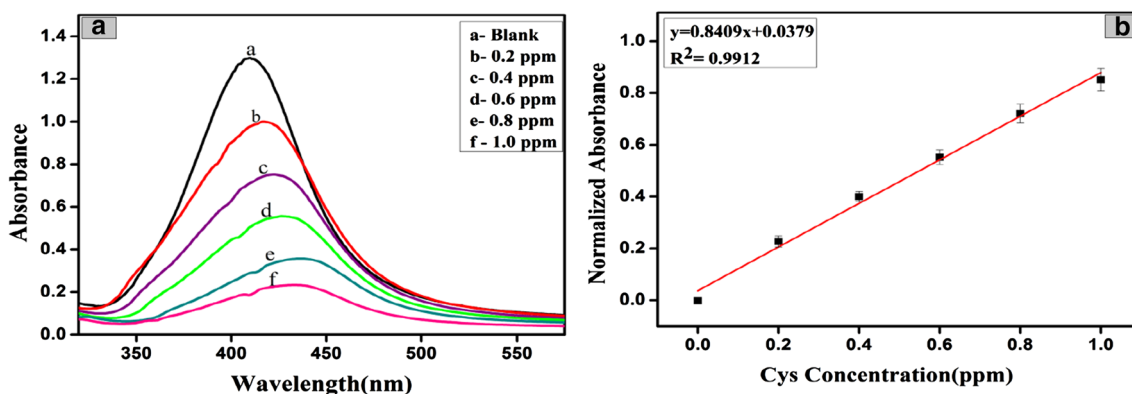

Fig. 7 **a** Absorption spectra of latex capped AgNPs with different concentrations of Cys (0.2–1.0 ppm) at pH 5.8, **b** Linear relationship between colorimetric response and Cys concentrations (0.2–1.0 ppm)
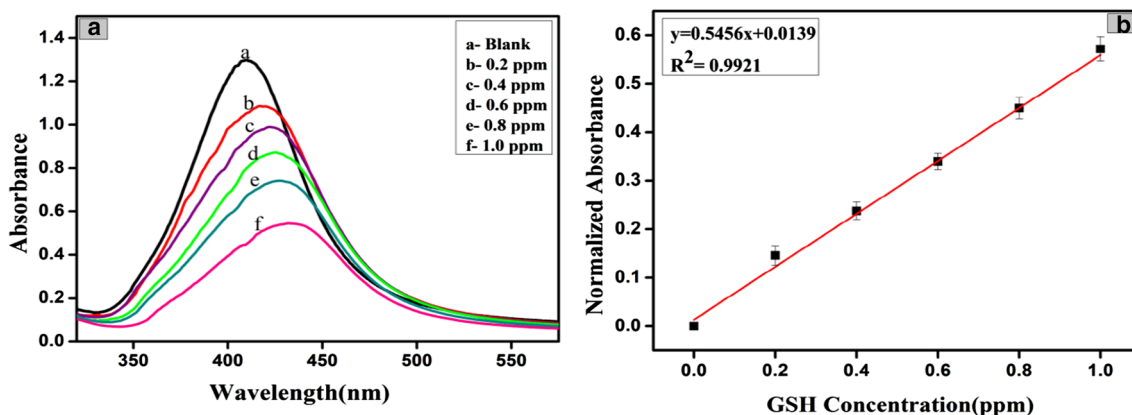

Fig. 8 **a** Absorption spectra of AgNPs with different concentrations of GSH (0.2–1.0 ppm) at pH 5.0, **b** Linear relationship between colorimetric response and GSH concentrations (0.2–1.0 ppm)

Table 1 Comparison of the proposed method with previously reported methods for the determination of Cys and GSH

Nanoparticles	Method	Linear dynamic range (ppm)	LOD (ppm)	Reference
Cys				
Polyvinylpyrrolidone-stablized AgNPs	UV–Visible	0.39–0.99	0.34	Bamdad et al. (2016)
Dextran coated AgNPs	UV–Visible	12.12–121.16	1.45	Davidović et al. (2017)
Ricinoleic acid coated AgNPs	UV–Visible	2.4–12.11	3.02	Viana et al. (2020)
Trisodium citrate capped Gold nanoparticles	UV–Visible	0.12–12.11	0.25	Nehzad et al. (2012)
Latex capped AgNPs	NDS	0.2–1.0	0.17	Present method
GSH				
GO-AgNPs	Chemiluminescent	9.22–307	7.68	He et al. (2012)
Rhodamin B-functionalized gold nanoparticles	Fluorescence	0.15–307	0.31	Cai et al. (2012)
Trisodium citrate capped Gold nanoparticles	UV–Visible	0.6–24.23	0.39	Hormozi-Nehzad et al. (2012)
Latex capped AgNPs	NDS	0.2–1.0	0.18	Present method

Table 2 Results of Cys recovery determination in blood and urine

Sample	Cys (ppm) added	Found value (ppm) $n = 3$	% Recovery	RSD $\pm$ %
Blood	0.4	0.395	98.75	0.92
	0.6	0.579	96.50	1.06
Urine	0.3	0.274	91.33	1.13
	0.7	0.646	92.21	0.98

Table 3 Results of GSH recovery determination in blood and urine

Sample	GSH (ppm) added	Found value (ppm) $n = 3$	% Recovery	RSD $\pm$ %
Blood	0.4	0.384	96.00	1.45
	0.6	0.575	95.83	0.95
Urine	0.3	0.275	91.65	0.91
	0.7	0.650	92.85	1.44

Table 4 Point and Interval Hypothesis test; Comparison of the proposed method with reference methods at 95% confidence level

Sample		Cys	GSH	Reference method (Cys)	Reference method (GSH)
Blood	% recovery[a]	98.75	95.83	99.30	96.40
	RSD	0.92	0.95	1.02	1.10
	t value[b]	1.26	2.12		
	F value[b]	1.30	1.41		
	θ_L	0.978	0.965		
	θ_U	1.040	1.070		
Urine	% recovery[a]	91.33	92.85	92.01	93.40
	RSD %	1.13	1.44	0.96	1.95
	t value[b]	2.25	1.20		
	F value[b]	1.31	1.92		
	θ_L[c]	0.972	0.981		
	θ_U[c]	1.060	1.093		

[a]Average for 3 independent analysis, [b]Tabulated t value ($\nu = 4$) = 2.776 and F value ($\nu_1 = 2$, $\nu_2 = 2$) = 19.00 for Cys (in blood and urine) and for GSH (in urine) at 95% confidence level. The tabulated t ($\nu = 9$) and F value ($\nu_1 = 7$, $\nu_2 = 2$) for GSH in blood are 2.262 and 19.35, respectively. [c]Bias, based on recovery experiments, of ± 2% is acceptable

It was also confirmed that no significance difference among the two methods.

Conclusion

We have developed a novel facile greener approach via the latex extract of *F. benghalensis* as a reducing and stabilizing agent for the production of AgNPs. The green synthesized latex capped AgNPs exhibit superior selectivity for GSH and Cys over the other biomolecules due to special interaction with the thiol group. The modern nanodrop

tabulated value at the 95% confidence level. The results are summarized in Table 4. Point and interval hypothesis test was also performed to calculate upper (θ_U) and lower acceptance limit (θ_L) (Rahman et al. 2016). The true bias based on the recovery experiments were measured using the following equation.

$$\theta^2 \left[\overline{X_1}^2 - S_P^2 t_{tab}^2 / n_1 \right] - 2\theta \overline{X_1} \overline{X_2} + \left[\overline{X_2}^2 + S_P^2 t_{tab}^2 / n_2 \right] = 0$$

where $\overline{X_1}$ and $\overline{X_2}$ are the average value determined by the proposed and reference methods, respectively. n_1 and n_2 are number of respective observations of proposed and reference method, respectively. S_p and t are the pooled standard deviation and one side t value at 95% confidence level, respectively. The values of θ_U and θ_L are reported in Table 4. The true bias was found to be less then ± 2% is acceptable.

spectrophotometer is being highly sensitive for the convenient analysis of biothiols in biological samples without matrix interferences. The ease of use, speed of measurement, lesser time analysis, microvolume quantity (0.5–1.0 µL) of the sample, and removal of cuvettes make this system suitable for accurate detection. Besides, our protocol is very simple and presents a good linear detection range at a low concentration of biothiols, compared with the previously reported method. Furthermore, the analytical performance of our proposed method was successfully applied in biological samples with good recoveries.

Compliance with ethical standards

Conflict of interest The authors declare there are no conflicts of interest.

References

Alothman ZA, Rahman N, Siddiqui MR (2013) Review on pharmaceutical impurities, stability studies and degradation products: an analytical approach. Rev Adv Sci Eng 2:155–166. https://doi.org/10.1166/rase.2013.1039

Amjadi M, Abolghasemi-Fakhri Z, Hallaj T (2015) Carbon dots-silver nanoparticles fluorescence resonance energy transfer system as a novel turn-on fluorescent probe for selective determination of cysteine. J photochem Photobiol A 309:8–14. https://doi.org/10.1016/j.jphotochem.2015.04.016

Aromal SA, Philip D (2012) Green synthesis of gold nanoparticles using trigonella foenum-graecum and its size-dependent catalytic activity. Spectrochim Acta, Part A 97:1–5. https://doi.org/10.1016/j.saa.2012.05.083

Bahram M, Mohammadzadeh E (2014) Green synthesis of gold nanoparticles with willow tree bark extract: a sensitive colourimetric sensor for cysteine detection. Anal Methods 6:6916–6924. https://doi.org/10.1039/C4AY01362J

Bamdad F, Khorram F, Samet M, Bamdad K, Sangi MR, Allahbakhshi F (2016) Spectrophotometric determination of L-cysteine by using polyvinylpyrrolidone-stabilized silver nanoparticles in the presence of barium ions. Spectrochim Acta, Part A 161:52–57. https://doi.org/10.1016/j.saa.2016.02.030

Bawaskar M, Gaikwad S, Ingle A, Rathod D, Gade A, Duran N, Marcato DP, Rai M (2010) A new report on mycosynthesis of silver nanoparticles by Fusarium culmorum. Curr Nanosci 6:376–380. https://doi.org/10.2174/157341310791658919

Cai HH, Wang H, Wang J, Wei W, Yang PH, Cai J (2012) Naked eye detection of glutathione in living cells using rhodamine B-functionalized gold nanoparticles coupled with FRET. Dyes Pigm 92:778–782. https://doi.org/10.1016/j.dyepig.2011.06.016

Christian GD (2007) Analytical Chemistry. Willey, Hoboken

Davidović S, Lazić V, Vukoje I, Papan J, Anhrenkiel SP, Dimitrijević S, Nedeljković JM (2017) Dextran coated silver nanoparticles—chemical sensor for selective cysteine detection. Colloids Surf B 160:184–191. https://doi.org/10.1016/j.colsurfb.2017.09.031

de Matos RA, da Silva Cordeiro T, Samad RE, Vieira ND Jr, Courrol LC (2011) Green synthesis of stable silver nanoparticles using Euphorbia milii latex. Colloids Surf A 389:134–137. https://doi.org/10.1016/j.colsurfa.2011.08.040

Deng R, Xie X, Vendrell M, Chang YT, Liu X (2011) Intracellular glutathione detection using MnO2-nanosheet-modified upconversion nanoparticles. Am Chem J 133:20168–201671. https://doi.org/10.1021/ja2100774

Desjardins P, Hansen JB, Allen M (2009) Microvolume protein concentration determination using the NanoDrop 2000c spectrophotometer. JoVE J Visualized Exp 33:1610. https://doi.org/10.3791/1610

Detsri E, Seeharaj P (2017) Colorimetric detection of glutathione based on phthalic acid assisted synthesis of silver nanoparticles. Colloids Surf A 533:125–132. https://doi.org/10.1016/j.colsurfa.2017.08.037

El-Rafie HM, El-Rafie M, Zahran MK (2013) Green synthesis of silver nanoparticles using polysaccharides extracted from marine macro algae. Carbohydr Polym 96:403–410. https://doi.org/10.1016/j.carbpol.2013.03.071

Guan X, Hoffman B, Dwivedi C, Matthees DP (2003) A simultaneous liquid chromatography/mass spectrometric assay of glutathione, cysteine, homocysteine and their disulfides in biological samples. J Pharm Biomed Anal 31:251–261. https://doi.org/10.1016/S0731-7085(02)00594-0

He Y, Cui H (2012) Synthesis of highly chemiluminescent graphene oxide/silver nanoparticle nano-composites and their analytical applications. J Mater Chem 22:9086–9091. https://doi.org/10.1039/C2JM16028E

Hormozi-Nezhad MR, Seyedhosseini E, Robatjazi H (2012) Spectrophotometric determination of glutathione and cysteine based on aggregation of colloidal gold nanoparticles. Sci Iran Trans F 19:958–963. https://doi.org/10.1016/j.scient.2012.04.018

Hsiao YP, Su WY, Cheng JR, Cheng SH (2011) Electrochemical determination of cysteine based on conducting polymers/gold nanoparticles hybrid nanocomposites. Electrochim Acta 56:6887–6895. https://doi.org/10.1016/j.electacta.2011.06.031

Huang GG, Hossain MK, Han XX, Ozaki Y (2009) A novel reversed reporting agent method for surface-enhanced Raman scattering; highly sensitive detection of glutathione in aqueous solutions. Analyst 134:2468–2474. https://doi.org/10.1039/B914976G

Ibrahim HM (2015) Green synthesis and characterization of silver nanoparticles using banana peel extract and their antimicrobial activity against representative microorganisms. J Radiat Res Appl Sci 8:265–275. https://doi.org/10.1016/j.jrras.2015.01.007

Kahrilas GA, Wally LM, Fredrick SJ, Hiskey M, Prieto AL, Owens JE (2014) Microwave-assisted green synthesis of silver nanoparticles using orange peel extract. ACS Sustain Chem Eng 2:367–376. https://doi.org/10.1021/sc4003664

Kalaiyarasan G, Hemlata C, Joseph J (2019) Fluorescence turn-on, specific detection of cystine in human blood plasma and urine samples by nitrogen-doped carbon quantum dots. ACS Omega 4:1007–1014. https://doi.org/10.1021/acsomega.8b03187

Khan MA, Khan T, Nadhman A (2016) Applications of plant terpenoids in the synthesis of colloidal silver nanoparticles. Adv Colloid Interface Sci 234:132–141. https://doi.org/10.1016/j.cis.2016.04.008

Li JF, Huang PC, Wu FY (2017) Specific pH effect for selective colorimetric assay of glutathione using anti-aggregation of label-free gold nanoparticles. RSC Adv 7:13426–13432. https://doi.org/10.1039/C7RA00399D

Li Y, Li Z, Gao Y, Gong A, Zhang Y, Hosmane NS, Shen Z, Wu A (2014) "Red-to-blue" colorimetric detection of cysteine via anti-etching of silver nanoprisms. Nanoscale 6:10631–10637. https://doi.org/10.1039/C4NR03309D

Liang SC, Wang H, Zhang ZM, Zhang X, Zhang HS (2002) Direct spectrofluorimetric determination of glutathione in biological

samples using 5-maleimidyl-2-(m-methylphenyl) benzoxazole. Anal Chim Acta 451:211–219. https://doi.org/10.1016/S0003-2670(01)01409-X

Mohammadi S, Khayatian G (2017) Colorimetric detection of biothiols based on aggregation of chitosan-stabilized silver nanoparticles. Spectrochim Acta 185:27–34. https://doi.org/10.1016/j.saa.2017.05.034

Nadagouda MN, Varma RS (2008) Green synthesis of Ag and Pd nanospheres, nanowires, and nanorods using vitamin: catalytic polymerisation of aniline and pyrrole. J Nanomater 2008:1–8. https://doi.org/10.1155/2008/782358

Patra S, Mukherjee S, Barui AK, Ganguly A, Sreedhar B, Patra CR (2015) Green synthesis, characterization of gold and silver nanoparticles and their potential application for cancer therapeutics. Mater Sci Eng 53:298–309. https://doi.org/10.1016/j.msec.2015.04.048

Potesil D, Petrlova J, Adam V, Vacek J, Klejdus B, Zehnalek J, Trnkova L, Havel L, Kizek R (2005) Simultaneous femtomole determination of cysteine, reduced and oxidized glutathione, and phytochelatin in maize (Zea mays L.) kernels using high-performance liquid chromatography with electrochemical detection. J Chromatogr A 1084:134–144. https://doi.org/10.1016/j.chroma.2005.06.019

Rahman N, Azmi SN, Wu HF (2006) The importance of impurity analysis in pharmaceutical products: an integrated approach. Accredit Qual Assur 11:69–74. https://doi.org/10.1007/s00769-006-0095-y

Rahman N, Sameen S, Kashif M (2016) Spectroscopic study on the interaction of haloperidol and 2, 4-dinitrophenylhydrazine and its application for the quantification in drug formulations. Anal Chem Lett 6:874–885. https://doi.org/10.1080/22297928.2016.1265898

Raj DR, Sudarsanakumar C (2017) Surface plasmon resonance based fiber optic sensor for the detection of cysteine using diosmin capped silver nanoparticles. Sens Actuators, A 253:41–48. https://doi.org/10.1016/j.sna.2016.11.019

Raoof JB, Ojani R, Kolbadinezhad M (2008) Voltammetric sensor for glutathione determination based on ferrocene-modified carbon paste electrode. J Solid State Electrochem 13:1411–1416. https://doi.org/10.1007/s10008-008-0690-4

Ravindran A, Chandrasekaran N, Mukherjee A (2012) Studies on differential behavior of silver nanoparticles towards thiol containing amino acids. Curr Nanosci 8:141–19. https://doi.org/10.2174/157341312799362331

Rout Y, Behera S, Ojha AK, Nayak PL (2012) Green synthesis of silver nanoparticles using Ocimum sanctum (Tulashi) and study of their antibacterial and antifungal activities. J Microbiol Antimicrob 4:103–109. https://doi.org/10.5897/JMA11.060

Saeb A, Alshammari AS, Al-Brahim H, Al-Rubeaan KA (2014) Production of silver nanoparticles with strong and stable antimicrobial activity against highly pathogenic and multidrug resistant bacteria. Sci World J 2014:1–9. https://doi.org/10.1155/2014/704708

Sathishkumar M, Sneha K, Won SW, Cho CW, Kim S, Yun YS (2009) Cinnamon zeylanicum bark extract and powder mediated green synthesis of nano-crystalline silver particles and its bactericidal activity. J Agric Food Chem 73:332–338. https://doi.org/10.1016/j.colsurfb.2009.06.005

Sharma A, Kumari M, Jagannadham MV (2009) Benghalensin, a highly stable serine protease from the latex of medicinal plant Ficus benghalensis. J Agric Food Chem 57:11120–11126

Siddiqui MR, AlOthman ZA, Rahman N (2017) Analytical techniques in pharmaceutical analysis: a review. Arabian J Chem 10:S1409–S1421. https://doi.org/10.1016/j.arabjc.2013.04.016

Song JY, Jang HK, Kim BS (2009) Biological synthesis of gold nanoparticles using Magnolia kobus and Diopyros kaki leaf extracts. Process Biochem 44:1133–1138. https://doi.org/10.1016/j.procbio.2009.06.005

Verma VC, Kharwar RN, Gange AC (2010) Biosynthesis of antimicrobial silver nanoparticles by the endophytic fungus Aspergillus clavatus. Nanomedicine 5:33–40. https://doi.org/10.2217/nnm.09.77

Viana AD, Nobrega ET, Moraes EP, Neto AO, Menezes FG, Gasparotto LH (2020) Castor oil derivatives in the environmentally friendly one-pot synthesis of silver nanoparticles: application in cysteine sensing. Mater Res Bull 124:110755. https://doi.org/10.1016/j.materresbull.2019.110755

Vinoth V, Wu JJ, Asiri AM, Anandan S (2017) Sonochemical synthesis of silver nanoparticles anchored reduced graphene oxide nanosheets for selective and sensitive detection of glutathione. Ultrason Sonochem 39:363–373. https://doi.org/10.1016/j.ultsonch.2017.04.035

Vishwasrao C, Momin B, Ananthanarayan L (2019) Green synthesis of silver nanoparticles using sapota fruit waste and evaluation of their antimicrobial activity. Waste Biomass Valorization 10:2353–2363. https://doi.org/10.1007/s12649-018-0230-0

Yadav YC, Srivastava DN, Saini V, Singhal S, Seth AK, Kumar S (2011) In-vitro antioxidant activity of methanolic extraction of Ficus Benghalensis L latex. Pharmacologyonline 1:140–148. https://doi.org/10.4172/2167-0501.1000216

Yang P, Chen Y, Zhu Q, Wang F, Wang L, Li Y (2008) Sensitive chemiluminescence method for the determination of glutathione, L-cysteine and 6-mercaptopurine. Microchim Acta 163:263–269. https://doi.org/10.1007/s00604-008-0006-5

Yuan X, Tay Y, Dou X, Luo Z, Leong DT, Xie J (2013) Glutathione-protected silver nanoclusters as cysteine-selective fluorometric and colorimetric probe. Anal Chem 85:1913–1919. https://doi.org/10.1021/ac3033678